Available online at www.sciencedirect.com
ScienceDirect
Cement and Concrete Research 38 (2008) 360–367
Cement and Concrete Research

An experimental, numerical and analytical investigation of gas flow characteristics in concrete

D.R. Gardner [a,1], A.D. Jefferson [b,*], R.J. Lark [b]

[a] Hyder Consulting (UK) Ltd. 10 Medawar Rd., The Surrey Research Park, Guildford, Surrey, GU2 7AR, UK
[b] Cardiff University School of Engineering, Queen's Buildings, The Parade, Cardiff CF24 3AA, UK

Received 6 June 2006; accepted 13 October 2007

Abstract

A series of tests are reported which used existing pressure cell apparatus to measure nitrogen gas flow in concrete. A finite difference numerical model is described which is used to investigate the time to reach steady state and the long-term transient response of the experimental system. An analytical solution is derived for the cell-pressure-time function from which a formula is derived for the intrinsic permeability coefficient. The permeabilities calculated from the experimental data have variations consistent with those from other investigations. The analytical solution matches the experimental pressure-time decay curves closely in the range of interest but there is a tendency for the curves to diverge for lower cell pressures. This is attributed to gas slippage and modifications to both the numerical and analytical solutions are described to account for this factor. Revised formulae are derived which give both the intrinsic permeability and Klinkenberg factor. These are then applied to the present experimental data and results compared with those from the literature.

Keywords: Permeability; Modelling; Gas flow; Concrete

1. Introduction

The modelling of flow processes in concrete and other cement-based materials is important when considering their long-term performance and durability [1,2]. In certain applications, such as nuclear containment vessels [3] and barrier structures in landfill sites [4], accurate modelling of flow processes is essential if required containment levels are to be maintained. Knowledge of the parameters that govern fluid flow in cementitious materials is therefore necessary if such accurate models are to be developed and used with confidence.

It is known that there is interaction between gas and moisture flow and that the apparent gas flow permeability varies with moisture content and pressure [5,6]. Nevertheless, the intrinsic permeability should be a material property applicable to all fluids for a given porous media, if corrections are made for gas slippage [7]. In general, it is easier to model gas, rather than liquid, flow through cement-based materials because their relatively low permeability makes testing with liquids very time consuming.

A number of laboratory based tests have been developed to measure the gas permeability of cement-based materials, including the CEMBUREAU test [3,8,9], the pressure cell method [10], the modified pressure cell method [11] and the Leeds permeability cell [12]. In-situ tests have also been developed [7,13–15]. It should be noted that in the related field of rock mechanics, permeability tests for cored samples have become standard [16].

As part of the extensive experimental programme of which the current work forms a part [17,18] investigations were undertaken using pressure cell apparatus similar to that used in Ref. [11]. The advantages of this method over other laboratory methods used for cementitious materials include the ability to test specimens of different size and geometry, relatively short specimen preparation and testing times and the fact that the permeability is based on a pressure range in a single test. A further advantage, realised in the present work, is that both the

* Corresponding author. Tel.: +44 29 20 874070.
E-mail address: JeffersonAD@cf.ac.uk (A.D. Jefferson).
[1] Formerly a post-graduate student at Cardiff University.

0008-8846/$ - see front matter © 2007 Elsevier Ltd. All rights reserved.
doi:10.1016/j.cemconres.2007.10.001

intrinsic permeability and Klinkenberg factor can be measured in a single test.

The aims of the work presented in this paper were to develop numerical and analytical procedures for the accurate simulation of the above tests, to derive expressions for the intrinsic permeability and Klinkenberg factor from cell-pressure-time measurements on cylindrical specimens and present results using the derived expressions from previously unpublished data.

In the CEMBUREAU test [8,9] the Hagen–Poiseuille equation is used to relate permeability to pressures and flow rates. Verdier et al. [3] explored the transient phase of the CEMBUREAU test using a one-dimensional finite difference model. In much previous work on cementitious materials using the present type of pressure cell an approximate exponential pressure-time function was used to calculate the permeability [10,11]. In the development of the modified Figg test, Claisse et al. [7,19] developed an analytical solution based on time varying one-dimensional radial gas flow and very recently Lafhaj et al. [20] have presented a study that compares in-situ and laboratory permeability results for limestone and concrete also using modified Figg test and an analytical solution essentially the same as that used by Claisse. Analytically based solutions have long been used to derive the properties from steady state [16] and transient tests [21] on rocks.

Much early work on developing solutions for gas flow problems was associated with the petroleum industry. As early as 1946 Muskat [22] developed an analytical method for transient gas flow problems based on successions of steady states and Russell in 1966 [23] developed the first accurate numerical solutions for gas well flow problems. In 1956 Carmen presented a monograph which includes a range of gas flow solutions based on Darcy's equation [24]. A summary of common test methods and associated analytical solutions is provided by Hall and Hoff [25].

In the present work a numerical model for transient one-dimensional radial flow is developed using finite difference approximations. A compact and convenient solution was developed in the visual mathematical programming environment Mathcad. This tool was then used to explore the transient response and time to reach steady state (t_{ss}) for a range of cylinder sizes. The fact that t_{ss} is short in comparison with the half time for cell-pressure decay meant that an accurate analytical solution could be developed based upon transient mass continuity conditions on the pressurised boundary of the cylindrical specimen and the steady state solution of gas flow through a cylinder. The solution to the resulting differential equation, although derived independently, is essentially similar to that developed for the modified Figg test [19,20].

Gas slippage, or the Klinkenberg effect, is known to significantly modify the apparent permeability, particularly at lower pressures [5,26,27], and in the present tests the effect was found to be significant. This effect has been ignored in much analytical and experimental work on porous materials but a series of solutions which allow for the Klinkenberg effect have been developed by Wu et al. [27].

One of the primary contributions of the present work is the derivation of expressions for both the intrinsic permeability and Klinkenberg factor in terms of the parameters measured by the present apparatus. These however used a different approximation from that used in the derivation of the transient solutions of Wu et al., primarily because of the relative simplicity of the final expressions derived from the present approach.

2. Experimental arrangement

The experimental procedure and the various series of tests conducted as part of this research programme are described in full by Gardner [17]. Here, only outline details of the tests

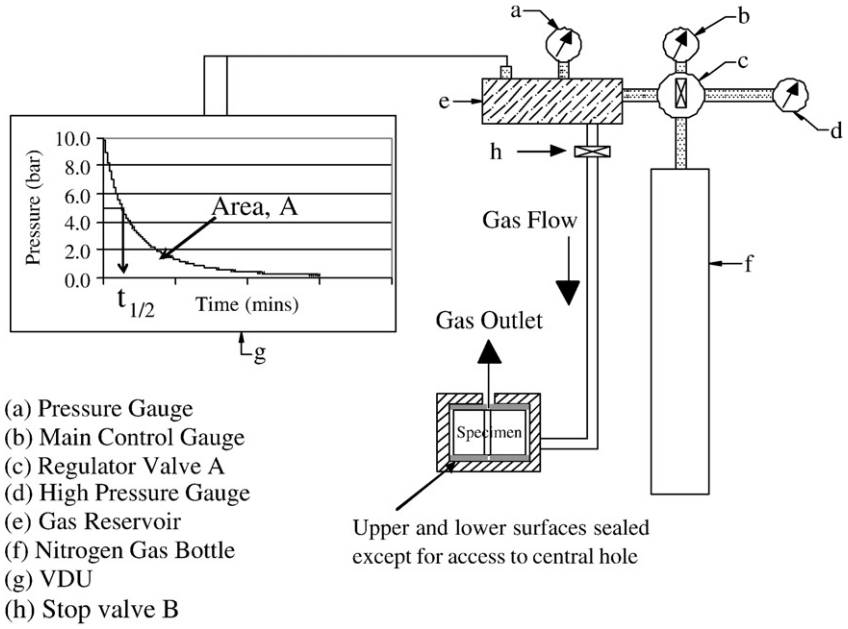

Fig. 1. Experimental apparatus.

Table 1
The effect of a change of model parameters on the time to reach steady state flow

θ	$k_{cf} \times 10^{-16}$	x_c	t_{ss}
0.06	2.0	0.05	13.1
0.04	2.0	0.05	9.8
0.02	2.0	0.05	5.1
0.06	6.0	0.05	5.1
0.06	1.0	0.05	24.4
0.06	0.8	0.05	30.5
0.06	2.0	0.025	3.7
0.06	2.0	0.037	7.8
0.06	2.0	0.062	20.3

considered in the modelling study will be provided. These comprise tests on cylindrical specimens with diameters 50 mm, 75 mm, 100 mm and 125 mm. The specimens were cored and cut from a series of 120 mm thick slabs, which had previously been cast and subsequently cured by wrapping in wet hessian for 7 days. Once cored, each specimen had a 6 mm hole drilled through the centre to full depth and then a 10 mm slice was cut from each end to produce specimens 100 mm in height. These were then conditioned in an oven at 105 °C, with conditioning being continued until the weight was effectively constant. Conditioning temperature was one of the factors investigated in the study [18] and it was found that there were insignificant differences in measured permeabilities between specimens conditioned at 85 °C and those conditioned at 105 °C, yet the latter stabilised in weight considerably sooner. It was thus concluded that concerns over significant damage occurring by curing at temperatures a little in excess of 100 °C were unfounded.

Two concrete mixes were used, one, denoted Normal Strength Concrete (NSC), with a mean 28 day cube strength of 44.5 N/mm^2 and the other, denoted C80, with a 28 day mean cube strength of 73 N/mm^2. Both used crushed limestone coarse aggregate with a maximum particle size of 10 mm. Six tests were performed for each size of cylinder for each mix, giving a total of 24 tests per mix. Each group of six tests is denoted by the mix and then the cylinder diameter, e.g. NSC125.

The experimental set up is illustrated in Fig. 1. The top and bottom surfaces of each specimen were sealed, except for the opening to the central hole, prior to the specimen being placed into the apparatus.

Nitrogen gas was stored in a pressurised cylinder, which was isolated from the test reservoir by the regulator valve A (see c Fig. 1). This valve was opened and a procedure of pressurising firstly the reservoir and then the remainder of the system was repeated until the pressure in the reservoir stabilised at 10 bar above atmospheric, at which point it was sealed from the pressurised gas cylinder by closing valve A. Each test was then started by opening valve B (see h Fig. 1). The tests were continued until the pressure in the reservoir had reduced to less than 4 bar above atmospheric (i.e. 501. kPa absolute). The 'half pressure' of 601 kPa is denoted $P_{1/2}$ and the time taken to reach this pressure $t_{1/2}$.

3. Modelling approach

3.1. Governing equations

A finite difference approach was adopted for the simulation of the gas flow experiments. The model developed was coded in a compact and transparent manner in the mathematical programming environment Mathcad. It is acknowledged that existing finite difference and finite element codes are available for modelling gas flow through porous media, but it proved more convenient to develop a bespoke model. This allowed the non-standard outer boundary condition, which depended on the volume of the reservoir, as well as gas-slippage effects, to be included readily. A brief description of the key governing equations and approach adopted for their solution are provided here. A full description of the numerical model and its validation are given by Gardner [17].

Considering one-dimensional flow only, and allowing for a change in area along the axis, the application of the mass-balance equation and Darcy's law leads to the following governing equation

$$-\frac{k_{ef}}{\theta\mu}\left[P\frac{\partial^2 P}{\partial x^2}A + P\frac{\partial P}{\partial x}\frac{\partial A}{\partial x} + \left(\frac{\partial P}{\partial x}\right)^2 A\right] + \frac{\partial P}{\partial t}A = 0 \qquad (1)$$

in which x=axial or radial coordinate (m), A=area normal to flow (m^2), P=pressure (N/m^2), μ=dynamic viscosity (kg m^{-1} s^{-1}), k_{ef}=intrinsic permeability (m^2) and θ is the connected porosity i.e. volume of connected pores/total volume.

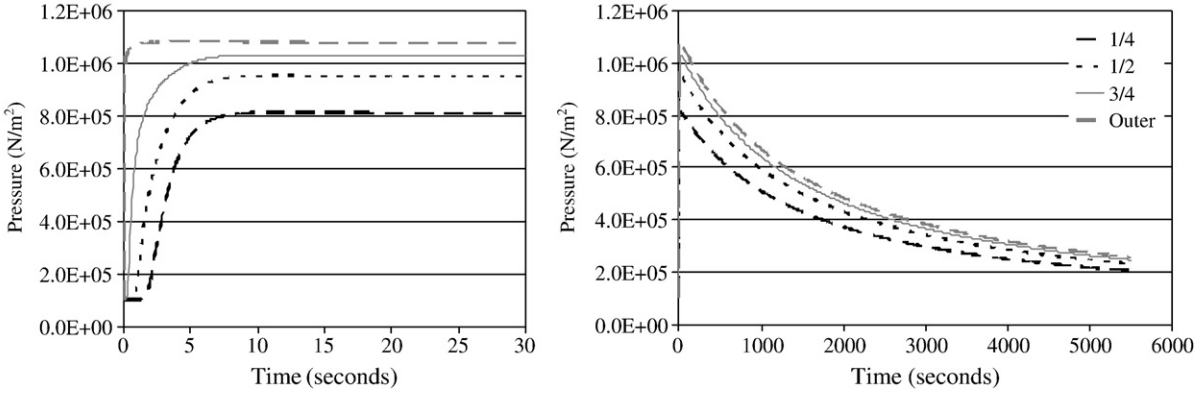

Fig. 2. Reservoir pressure-time diagrams at different radii for two time scales.

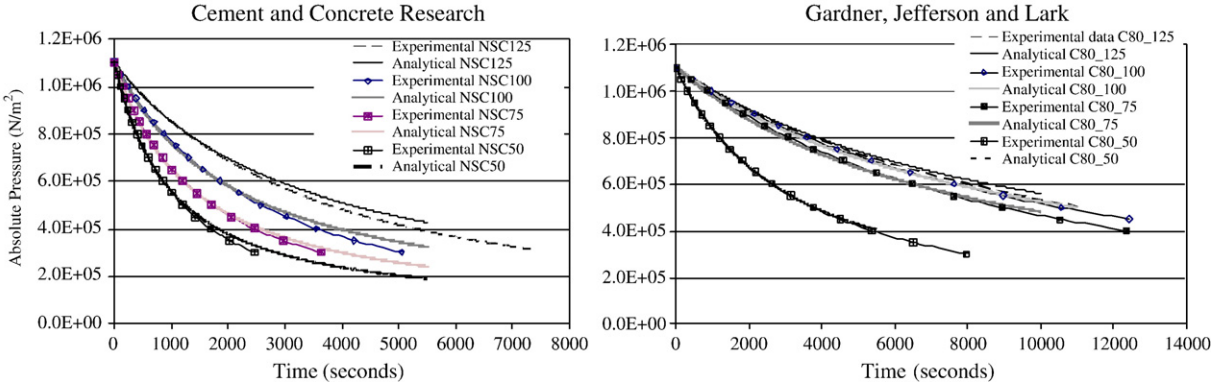

Fig. 3. Analytical and experimental reservoir pressure v time responses.

3.2. Numerical solution

The numerical solution assumes radial flow conditions. The following governing differential equation is obtained from Eq. (1) by replacing A with $2\pi xh$ where h is the height of the flow path

$$C_a \frac{\partial P}{\partial x} + C_b \frac{\partial^2 P}{\partial x^2} - x\frac{\partial P}{\partial t} = 0 \tag{2}$$

in which $C_a = \frac{k^{ef}}{\theta\mu}\left(P + x\frac{\partial P}{\partial x}\right)$ and $C_b = \frac{k^{ef}}{\theta\mu}Px$. Central finite difference approximations were applied for spatial discretisation and a generalised two-level scheme applied for the temporal discretisation [28], in which the point within a time interval at which the equations are considered is governed by the parameter r (where $0 \le r \le 1$)

$$\mathbf{p}_{t+r\Delta t} = (1-r)\mathbf{p}_t + r\mathbf{p}_{t+\Delta t} \tag{3}$$

in which $\mathbf{p}_t$ is the vector of grid point pressures at time t. The parameters C_a and C_b vary with pressure, which would suggest that an implicit time-stepping scheme is necessary. However, it was found in all cases considered that a grid and time-step converged solution could be obtained quickly without iteration within a time interval using $r=0.9$.

3.3. Time to reach steady state conditions

The time to reach steady state (t_{ss}) is important in the current work since the analytical solution given in the following subsection of this paper is only valid if t_{ss} is small relative to the time it takes for a significant decay in cell pressure. Hence, a study was performed to test the sensitivity of $t_{1/2}$ to the intrinsic permeability, volumetric gas constant and radius of specimen analysed. Comparison is made with the radial steady state analytical solution with fixed pressures on either boundary [16,19,20];

$$P = \sqrt{C\ln(x) + D} \tag{4}$$

in which $C = \frac{P_c^2 - P_h^2}{\ln(x_c/x_h)}$ and $D = P_h^2 - \left[\frac{\left(P_c^2 - P_h^2\right)}{\ln(x_c/x_h)}\right]\ln x_h$, in which x_h and x_c are the radii of the central hole and outside of cylinder respectively, and P_h and P_c the associated pressures.

The assumed boundary conditions were $P_c = 1013$ kPa and P_h = atmospheric. Steady state conditions were judged to have been reached when no point changed in pressure by more than 0.01% of the peak pressure over six time steps. The results from this study are summarised in Table 1. It was found that the shortest time in any experiment for the applied pressure to decay to half the original was over 1000 s, thus in all cases it may be seen that t_{ss} is very small by comparison.

3.4. Numerical simulation of pressure decay permeability test

The following equation, which governs the outer boundary condition for the pressure decay permeability test, is derived by considering the mass balance between the gas exiting the reservoir and entering the cylindrical specimen

$$V_0 \frac{\partial P}{\partial t} = 2\pi x_c h\left(-k_{ef}\frac{P}{\mu}\right)\frac{\partial P}{\partial x} \tag{5}$$

in which V_0 is the combined volume of the reservoir and the gas surrounding the specimen.

The experiment is typically continued for 5500 s and in the analysis two time scales are observable, the first is very close to the time to reach steady state conditions in the cylinder for fixed pressure boundary conditions, and the second is associated with the pressure decay in the reservoir. Fig. 2 presents the numerical results with pressures at the outer boundary and three internal positions included.

Table 2
Calculated Intrinsic permeabilities

Test ref	Path length (mm)	Average $k_{ef} \times 10^{-17}$ m^2	F3T $k_{ef} \times 10^{-17}$ m^2	V%
NSC50	22.0	17.1	23.0	31.3
NSC75	34.5	14.6	19.4	23.1
NSC100	47.0	11.9	14.0	23.4
NSC125	59.5	11.8	10.4	26.5
C80_50	22.0	5.9	7.5	38.1
C80_75	34.5	3.4	3.6	4.7
C80_100	47.0	3.4	3.5	4.7
C80_125	59.5	3.2	3.5	16.9

Table 3
Intrinsic permeabilities and Klinkenberg factors

Spec	$\frac{t_{1/2}}{t_{3/4}}$	$k_i \times 10^{-1}$ m^2	b kPa
NSC50	2.71	19.3	174
NSC75	2.78	17.9	78
NSC100	2.69	11.3	215
NSC125	2.70	8.5	204
C80_50	2.83	7.3	17
C80_75	2.66	2.8	269
C80_100	2.66	2.7	259
C80_125	2.74	3.0	131

3.5. Analytical transient solution

The fact that the time to steady state is so much smaller than the time for the reservoir pressure to decay to half the starting value, suggests that a relatively accurate analytical solution can be derived using the steady state solution for flow through the cylinder and the mass continuity equation at the outer boundary. This may be thought of as continuous successions of steady states as in the original work of Muskat [22]. The resulting governing equation becomes;

$$\frac{\partial P_c}{\partial t} + C_\alpha P_c^2 - C_\beta = 0 \tag{6}$$

in which $C_\alpha = \frac{1}{C_v 2x_c \ln(x_c/x_h)}$, $C_\beta = \frac{P_h^2}{C_v 2x_c \ln(x_c/x_h)}$ and $C_v = \frac{V_0 \mu}{2\pi x_c h k_{ef}}$
A solution to Eq. (6) is as follows

$$P_c = P_h \operatorname{cotanh}(\beta t + \gamma) \tag{7}$$

in which $\beta = \frac{P_{atm}}{C_v 2x_c \ln(x_c/x_h)}$ and $\gamma = \operatorname{cotanh}^{-1}\left(\frac{P_{c_0}}{P_{atm}}\right)$ Eq. (7) can be rearranged to give an expression in terms of k_{ef} and $t_{1/2}$, as follows

$$k_{ef} = \frac{\ln\left[\frac{(P_{1/2}+P_{atm})(P_{c_0}-P_{atm})}{(P_{1/2}-P_{atm})(P_{c_0}+P_{atm})}\right]}{2t_{1/2}\pi h P_{atm}} V_0 \mu \ln(x_c/x_h) \tag{8}$$

noting that for an arbitary scalar z, $\operatorname{cotanh}(z) = \frac{1}{2}\ln\left(\frac{z+1}{z-1}\right)$. It is noted that the solution is essentially similar to that given for the modified Figg test [19,20].

4. Comparison with experimental data

In this section comparisons are shown between the results from experiments described in Section 2 of this paper and results from the analytical solution described in Section 4. The numerical and analytical solutions are indistinguishable for the parameters used in these tests and therefore only the analytical solutions are plotted. Each experiment, with a given mix and specimen size, was carried out 6 times, and the experimental results shown here in Fig. 3 are those for the experiment in the group with the effective permeability nearest to the mean of the group. The analytical results were obtained from Eq. (7) using the permeability value appropriate for the experiment as calculated from Eq. (8).

Table 2 shows the average mean intrinsic permeability from each group, the value specific to the test plotted in Fig. 3 (denoted F3T), the gas path lengths and coefficients of variation (V%) from each group.

Firstly, the graphs show the expected result that the stronger concrete has a lower permeability. The analytical response curves are acceptably close to those from the experimental data, although the curves noticeably diverge as the pressure reduces, particularly for the NSC specimens. The maximum discrepancy at time $t_{1/2}$ is 6% relative to the experimental data. It is noted that the values specific to the tests considered in Fig. 6 were used and these differ slightly from the average values quoted in Table 3. The divergence at lower pressures is thought to be due to gas slippage, the effects of which are explored in the next section of this paper.

It is well-known that measured permeabilities are subject to a significant degree of variation and the results shown in Table 3 are considered to have acceptable degrees of consistency when compared with those obtained by other workers [3,5,14]. However, there does appear to be a trend that the average intrinsic permeability decreases as the size of the specimen increases. There could be a number of reasons for this, one of which is that the effects of damage near the boundaries due to coring become proportionally less as the specimen size increases. Also, the maximum aggregate size of 10 mm is approximately one half the gas path length for the smallest specimens, which means that the smaller specimens may not be

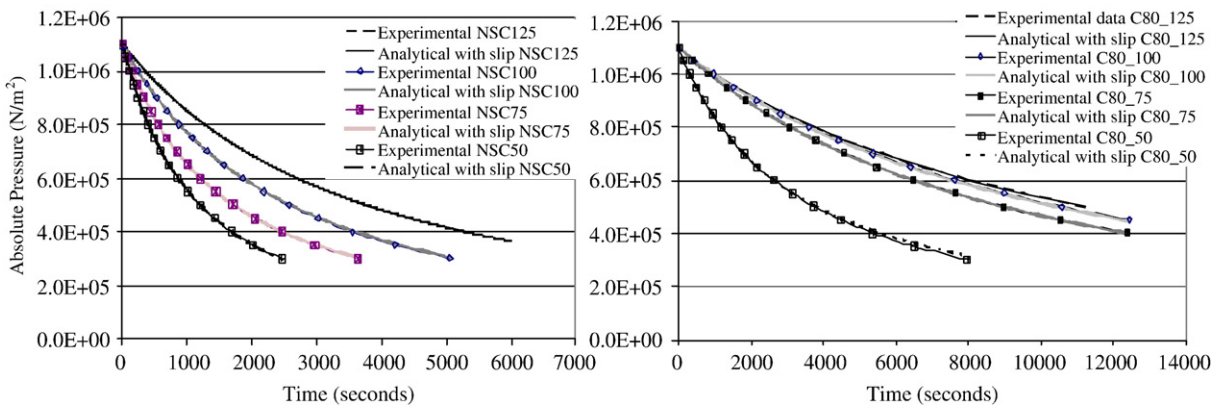

Fig. 4. Analytical with slip and experimental reservoir pressure v time responses.

Table 4
Comparison with intrinsic gas permeabilities from other authors

Ref	Detail	k_{ef} (m^2)	k_i (m^2)
Present work NSC		10.4E−17 to 23.0E−17	8.5E−17 to 19.3E−17
Present work C80		3.5E−17 to 7.5E−17	2.7E−17 to 7.3E−17
Verdier et al. [3]	C62 Concrete with gravel aggregate at pressure diff. 0.4 MPa	5.2E−17	
Monlouis–Bonnaire et al. [6]	C62 Gravel and limestone aggregate concrete at pressure diff 1 bar. 0% saturation case	22E−17 to 28E−17	
Claisse et al. [7]	Vacuum test on various concrete with quartzitic uncrushed aggregate	0.45E−17 to 10E−17	
Bamforth [5]	High strength, light weight, air entrained and PFA concretes	0.1E−17 to 1.3E−17	3.58E−20 to 2.39E−18

as representative of the average properties as the largest mixes. A further reason may be associated with gas slippage, an issue which will be assessed in the following section.

5. Simulating gas-slippage effects

A consequence of gas slippage is that the apparent gas permeability k_{ef} is greater than the true intrinsic permeability k_i [5,26,27,29]. This so called Klinkenberg effect [26] may be taken into account by modifying the permeability as follows

$$k_{ef} = k_i\left(1+\frac{b}{P}\right) \tag{9}$$

in which b is the Klinkenberg factor with units of pressure and k_i is the absolute permeability.

Wu et al. [27] showed that analytical expressions accounting for the Klinkenberg effect could be derived by using the standard form of governing mass-balance equation (e.g. Eq. (1)) but with P replaced by a transformed variable $P_b=P+b$. They also showed that for transient solutions the approximation of using a constant average pressure to compute the effective permeability is necessary to linearise the governing equation. Thus, the solutions already derived could be used directly with the transformed variable and an averaged permeability to allow for the Klinkenberg effect. However, it proved that an accurate equation and more convenient final expressions for k_i and b could be derived by applying an averaging factor (a) to the Klinkenberg modified permeability and using this directly in analytical solution, as follows;

$$P_c = P_{atm}\ \text{cotanh}\left(\chi k_i\left(1+a\frac{b}{P_c}\right)t+\gamma\right) \tag{10}$$

in which $\chi=\frac{P_{atm}\pi h}{\ln\left(\frac{x_c}{x_h}\right)V_0\mu}$ and $a=2/3$

This equation was found to give results that were indistinguishable (within 1%) from the Klinkenberg modified numerical solutions for the tests considered below and it was deemed therefore to have sufficient accuracy.

If, in addition to ($t=t_{1/2}$, $P_c=P_{1/2}$), a second point ($t=t_{3/4}$, $P_c=P_{3/4}$) is taken from the experimental time–pressure curve, where $P_{3/4}=851$ kPa and $t_{3/4}$ is the time taken to reach $P_{3/4}$, then Eq. (10) can be solved for b and k_i as follows

$$b=\frac{\frac{t_{1/2}}{t_{3/4}}-\frac{c_{1/2}}{c_{3/4}}}{a\left(\frac{c_{1/2}}{c_{3/4}}\frac{1}{P_{3/4}}-\frac{t_{1/2}}{t_{3/4}}\frac{1}{P_{1/2}}\right)} \tag{11}$$

$$k_i=\frac{c_{1/2}}{\chi t_{1/2}\left(1+a\frac{b}{P_{1/2}}\right)} \tag{12}$$

in which $c_i=\text{cotanh}^{-1}\left(\frac{P_i}{P_{atm}}\right)-\gamma$. Values of k_i and b calculated using Eqs. (11) and (12) for the 8 experiments considered in Fig. 3 are shown in Table 3 and solutions using Eq. (10) are compared with these same experimental data in Fig. 4.

It may be seen from Fig. 4 that the analytical expressions are now all but indistinguishable from the experimental data.

Table 4 gives comparisons with results from other authors. This shows that the present values are reasonable although the permeabilities are relatively high. Contributory factors to this may include the relatively high permeability of the limestone aggregate used in the production of the concrete and the complete dryness of the present specimens. The latter point is particularly relevant because it has been shown that even small amounts of moisture reduce the gas permeability significantly [6,30] and many of the quoted permeability values have been obtained for concrete specimens that have not been conditioned by heating e.g. Ref. [5].

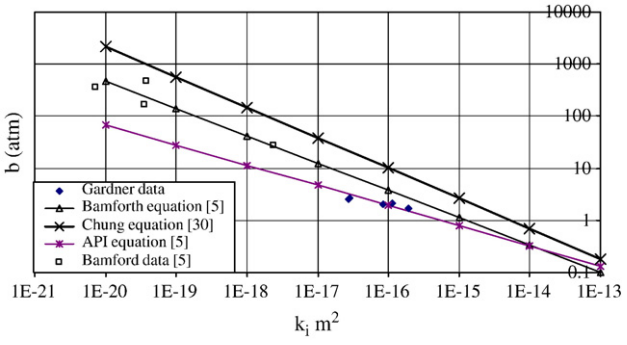

Fig. 5. Slip flow constant (b) vs gas permeability.

Klinkenberg's slip constant is known to vary with permeability [26,5,30]. Bamford [5] and more recently Chung et al. [30] have proposed relationships between k_i and b for concrete and some fifty years ago the American Petroleum Institute (discussed by Bamford [5]) provided a relationship derived for oil sands. A plot showing these relationships along with the present data is shown in Fig. 5. It may be seen that if the out lying data points are omitted from the plot, these present data fit API equation reasonably well. However, for the present high permeability materials, the differences between k_{ef} and k_i are relatively small and consequentially the values for b are particularly sensitive to the ratio and the variation in the b values obtained are relatively high. This sensitivity precludes a strong conclusion regarding the applicability of the API equation to the present dry high permeability concrete.

6. Conclusions

The permeability results from the two experimental test series on cylindrical specimens considered in this work had variations consistent with those of similar tests by other authors.

The apparatus used has the advantage that it can test specimens of different sizes and the advantage that both a permeability and Klinkenberg factor can be obtained from a single test.

The transient finite difference Mathcad worksheet developed for modelling the test specimens was compact and convenient, and gave results which closely matched the experimental data.

The transient gas flow response through the test specimens exhibited two time scales, one associated with the time to reach steady state and the other associated with the time taken for the cell pressure to decay to one half of the original value, i.e. the half time. It is concluded that, for all practical sizes of cement-based specimens, the time to steady state is always much shorter than the half time. This conclusion allowed an accurate transient analytical solution to be derived based upon a one-dimensional radial steady state flow equation and the mass-balance equation between gas exiting the reservoir and that entering the cylinder. The match between results from this analytical solution and the numerical model is extremely close for all cases considered. From this analytical solution, a formula was derived that gives the intrinsic permeability in terms of the half time. This analytically based formula is considered a significant improvement on the empirically based formulae used by previous workers with the present apparatus on cementitious materials.

Although the analytical pressure curves were close to the experimental, there was a tendency for the curves to diverge at lower pressures. This was attributed to gas slippage, i.e. the Klinkenberg effect, and the numerical and analytical procedures were therefore modified to account for this. A method was derived to compute both the intrinsic permeability and the Klinkenberg factor from a single test. The match between numerical, analytical and experimental results was then extremely close for all tests considered.

The final results showed that the present intrinsic permeability values were within the bounds of those from others workers albeit that they are at the upper end of the spectrum. The likely reason for this is the complete dryness of the specimens achieved by the present heating process. This is relevant because permeability has been shown to increase rapidly with moisture content and much of the data in the literature has been obtained for concrete which has not been dried by heating.

The Klinkenberg slip factor was found to vary with intrinsic permeability as found by other authors. The present data were found to match reasonably the relationship proposed by the API but the high sensitivity of the slip factor to the measured time ratio in this permeability range precludes a general conclusion that the API equation is applicable to high permeability concrete based on these data alone.

References

[1] G. Meshke, S. Grasberger, Thermo-hygro-mechanical degradation of concrete: From coupled 3D material modelling to durability-orientated multifield structural analyses, Materials and Structures 37 (2004) 244–256.
[2] L. Sanavia, F. Pesavento, B.A. Schrefler, Finite element analysis of non-isothermal multiphase geomaterials with application to strain localization simulation, Computational Mechanics 37 (4) (2006) 331–348.
[3] J. Verdier, M. Carcassès, Modelling of a gas flow measurement: application to nuclear containment vessels, Cement and Concrete Research 32 (8) (2002) 1331–1340.
[4] P.A. Claisse, E. Ganjian, A. Atkinson, M. Tyrer, Measuring and predicting transport in composite cementitious barriers, ACI Materials Journal 103 (2) (2006) 113–120.
[5] P.B. Bamforth, The relationship between permeability coefficients for concrete obtained using liquid and gas, Magazine of Concrete Research 39 (138) (1987) 3–11.
[6] J.P. Monlouis-Bonnaire, J. Verdier, B. Perrin, Prediction of the relative permeability to gas flow of cement based materials, Cement and Concrete Research 34 (5) (2004) 737–744.
[7] P.A. Claisse, E. Ganjian, T.A. Adlam, A vacuum permeability test for in situ assessment of cover concrete, Cement and Concrete Research 33 (2003) 47–53.
[8] J.J. Kollek, The determination of the permeability of concrete to oxygen by the Cembureau method — a recommendation, Materials and Structures 22 (1989) 225–230.
[9] A. Abbas, M. Carcassès, J.-P. Ollivier, Gas permeability of concrete in relation to its degree of saturation, Materials and Structures 32 (1999) 3–8.
[10] G.R. Martin, A method for determining the relative permeability of concrete using gas, Magazine of Concrete Research 38 (135) (1986) 90–94.
[11] F.D. Lydon, The relative permeability of concrete using nitrogen gas, Construction and Building Materials 7 (4) (1993) 213–220.
[12] J.G. Cabrera, C.J. Lynsdale, A new gas permeameter for measuring the permeability of mortar and concrete, Magazine of Concrete Research 40 (144) (1988).
[13] J.W. Figg, Methods of measuring the air and water permeability of concrete, Magazine of Concrete Research 25(85) 213–219.
[14] P.A.M. Basheer, A.E. Long, F.R. Montgomery, The Autoclam — a new test for permeability, Concrete (July/August 1994) 27–29.
[15] R.K. Dhir, P.C. Hewlett, E.A. Byars, I.G. Shaaban, A new technique for measuring the air permeability of near-surface concrete source, Magazine of Concrete Research 47 (171) (1995) 167–176.
[16] ASTM, ASTM Rock testing handbook, http://www.wes.army.mil/SL/MTC/handbook/RT/RockTestingHandbook.htm July 2007Accessed.
[17] D.R. Gardner, Experimental and numerical studies of the permeability of concrete, PhD Thesis, Cardiff University, UK, (2005).
[18] D.R. Gardner, R.J. Lark, B. Barr, Effect of condition temperature on the strength and permeability of normal- and high-strength concrete, Cement and Concrete Research 25 (2005) 1400–1406.

[19] P.A. Claisse, H.I. Elsayad, I.G. Shaaban, Test methods for measuring fluid transport in cover concrete, Journal of Materials in Civil Engineering 11 (2) (1999) 138–143.
[20] Z. Lafhaj, G. Richard, M. Kaczmarel, F. Skoczlas, Experimental determination of intrinsic permeability of limestone and concrete: comparison between insitu and laboratory results, Building and Environment 42 (2007) 3042–3050.
[21] P.A. Hsieh, J.V. Tracy, C.E. Neuzil, J.D. Bredehoeft, S.E. Silliman, A transient laboratory method for determining the hydraulic properties of 'tight' rocks — I Theory, International Journal of Rock Mechanics and Mining Sciences & Geomechanics Abstracts 18 (1981) 245–252.
[22] M. Muskat, The Flow of Homogeneous Fluids through Porous Media, Edwards, Ann Arbor.
[23] D.G. Russell, J.H. Goodrich, J.F. Perry, Method for predicting gas well performance, Journal of Petroleum Technology (1966) 99–108.
[24] P.C. Carmen, Flow of gases through porous media, Butterworths, London, 1956.
[25] C. Hall, W.D. Hoff, Water transport in brick, stone and concrete, Taylor and Francis, 2002.
[26] L.J. Klinkenberg, The permeability of porous media to liquids and gases, Drilling Production Practice, American Petroleum Institute, New York, 1941, pp. 200–213.
[27] Y.-S. Wu, K. Pruess, P. Persoff, Gas flow in porous media with Klinkenberg effects, Transport in Porous Media 32 (1998) 117–137.
[28] O.C. Zienkiewicz, K. Morgan, Finite elements and approximations, John Wiley, 1983.
[29] M. Lion, F. Skoczylas, L. Lafhaj, M. Sersar, Experimental study on mortar. Temperature effects on porosity and permeability. Residual properties or direct measurements under temperature, Cement and Concrete Research 35 (2005) 1937–1942.
[30] J.H. Chung, G.R. Consolazio, Numerical modelling of transport phenomena in reinforced concrete exposed to elevated temperatures, Cement and Concrete Research 35 (2005) 597–608.